O–H Bond Cleavage

International Edition: DOI: 10.1002/anie.201505336
German Edition: DOI: 10.1002/ange.201505336

On the Mechanisms of Hydrogen-Atom Transfer from Water to the Heteronuclear Oxide Cluster $[Ga_2Mg_2O_5]^{\bullet+}$: Remarkable Electronic Structure Effects

*Jilai Li, Shaodong Zhou, Xiao-Nan Wu, Shiya Tang, Maria Schlangen, and Helmut Schwarz**

Dedicated to Professor Peter Schwerdtfeger on the occasion of his 60th birthday

Abstract: *Mechanistic insight into the homolytic cleavage of the O–H bond of water by the heteronuclear oxide cluster $[Ga_2Mg_2O_5]^{\bullet+}$ has been derived from state-of-the-art gas-phase experiments in conjunction with quantum chemical calculations. Three pathways have been identified computationally. In addition to the conventional hydrogen-atom transfer (HAT) to the radical center of a bridging oxygen atom, two mechanistically distinct proton-coupled electron-transfer (PCET) processes have been identified. The energetically most favored path involves initial coordination of the incoming water ligand to a magnesium atom followed by an intramolecular proton transfer to the lone-pair of the bridging oxygen atom. This step, which is accomplished by an electronic reorganization, generates two structurally equivalent OH groups either of which can be liberated, in agreement with labeling experiments.*

Water is the most ubiquitous compound on earth, and sunlight-initiated efficient water splitting is regarded as the holy grail in the context of a sustainable hydrogen-based economy.[1] Metal oxides are considered as promising catalysts for water oxidation.[2] Further, cleavage of the O–H bond in water by transition-metal compounds results in the generation of valuable metal hydroxides or metal alkoxides. The mechanistic understanding of how water interacts with metal oxides is of fundamental importance, but still far from being complete.[3]

The ultimate goal in heterogeneous catalysis is, in the extreme, to perform single-atom catalysis (SAC),[4] and gas-phase clusters have been considered to serve as ideal models to probe the active site of a catalyst.[5] Herein, a detailed investigation on the reactivity of the heteronuclear oxide cluster $[Ga_2Mg_2O_5]^{\bullet+}$ toward water in the gas phase has been conducted by state-of-the-art mass-spectrometry based experiments in conjunction with quantum chemical (QC) calculations.[6] As shown earlier, the mechanistic understanding derived from these investigations provides fundamental concepts and may guide in the rational design of low-molecular-weight catalysts.[5b–h,7]

The Fourier transform ion-cyclotron resonance (FT-ICR) mass spectra, Figure 1, show the reactions of mass-selected,

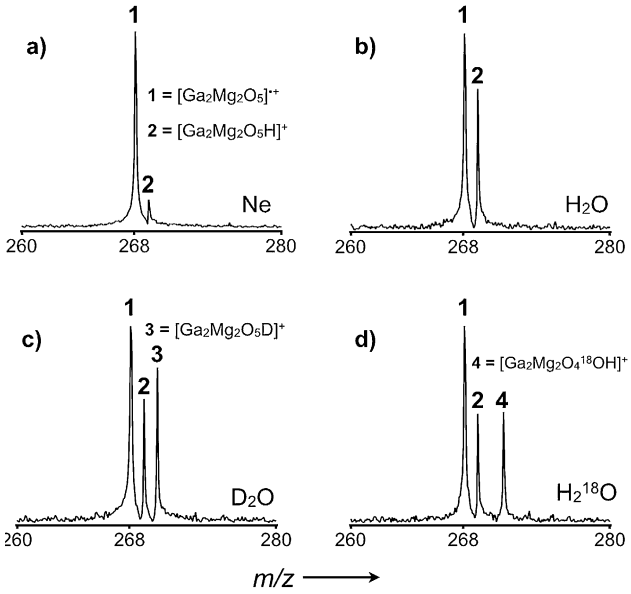

Figure 1. Mass spectra showing the reactions of mass-selected $[Ga_2Mg_2O_5]^{\bullet+}$ with a) Ne at a pressure of approximately 1.0×10^{-9} mbar, b) H_2O at a pressure of approximately 1.3×10^{-9} mbar, c) D_2O-enriched water at a pressure of approximately 2.4×10^{-9} mbar, and d) $H_2{}^{18}O$ at a pressure of approximately 2.0×10^{-9} mbar after a reaction delay of 3 seconds. See text for details and Supporting Information for a larger mass range.

thermalized $[Ga_2Mg_2O_5]^{\bullet+}$ ions (*m*/*z* 268, see Ref. [7a] for details) with water and its isotopomers; the reaction with Ne has also been recorded to provide a reference spectrum. As shown in Figure 1a, the hydrogen-atom transfer (HAT) product ion $[Ga_2Mg_2O_5H]^+$ is formed even if the ICR cell is filled only with neon, that is, $[Ga_2Mg_2O_5]^{\bullet+}$ reacts with background impurities. However, the intensity of the product ion $[Ga_2Mg_2O_5H]^+$ is much higher when H_2O is leaked into the ICR cell (Figure 1b, and Reaction (1)). The O–H bond scission was confirmed in an isotopic labeling experiment with D_2O-enriched water, in which the product ion $[Ga_2Mg_2O_5D]^+$ is observed (Figure 1c, Reaction (2)). When labeled $H_2{}^{18}O$ is

[*] Dr. J. Li, Dr. S. Zhou, Dr. X.-N. Wu, Dr. S. Tang, Dr. M. Schlangen, Prof. Dr. H. Schwarz
Institut für Chemie, Technische Universität Berlin
Strasse des 17. Juni 135, 10623 Berlin (Germany)
E-mail: Helmut.Schwarz@tu-berlin.de
Dr. J. Li
Institute of Theoretical Chemistry, Jilin University
Changchun 130023 (P.R. China)

Supporting information for this article is available on the WWW under http://dx.doi.org/10.1002/anie.201505336.

introduced in the ICR cell, in addition to a signal for $[Ga_2Mg_2O_5H]^+$, a signal with $\Delta m = +3$ relative to the precursor $[Ga_2Mg_2O_5]^{\bullet+}$ appears (Figure 1d; Reactions (3) and (4)). The presence of $[Ga_2Mg_2O_4{}^{18}OH]^+$ indicates an oxygen-atom exchange between $H_2{}^{18}O$ and the oxide cluster (Reaction (3)). All these product ions are formed in primary reactions as revealed by double-resonance experiments. For example, constant removal of the product ion $[Ga_2Mg_2O_5H]^+$ from the reaction cell does not affect the formation of $[Ga_2Mg_2O_4{}^{18}OH]^+$. The rate constant $k([Ga_2Mg_2O_5]^{\bullet+}/H_2O)$ is estimated to 6.6×10^{-10} cm^3 molecule^{-1} s^{-1}, corresponding to a collision efficiency of $\phi = 37\%$, relative to collision rate calculated with average-dipole orientation theory.[8] Summarizing the experimental findings, it is clear that $[Ga_2Mg_2O_5]^{\bullet+}$ activates water under thermal conditions.

$$[Ga_2Mg_2O_5]^{\bullet+} + H_2O \longrightarrow [Ga_2Mg_2O_5H]^+ + HO^{\bullet} \quad (1)$$

$$[Ga_2Mg_2O_5]^{\bullet+} + D_2O \longrightarrow [Ga_2Mg_2O_5D]^+ + DO^{\bullet} \quad (2)$$

$$[Ga_2Mg_2O_5]^{\bullet+} + H_2{}^{18}O \longrightarrow [Ga_2Mg_2O_4{}^{18}OH]^+ + HO^{\bullet} \quad (3)$$

$$[Ga_2Mg_2O_5]^{\bullet+} + H_2{}^{18}O \longrightarrow [Ga_2Mg_2O_5H]^+ + H^{18}O^{\bullet} \quad (4)$$

To obtain mechanistic insight in the $[Ga_2Mg_2O_5]^{\bullet+}$ mediated activation of H_2O, QC calculations have been performed;[6c] the potential energy surfaces (PESs) are shown in Figure 2, and the corresponding structural parameters are given in Table 1.

As shown in Figure 2, three different pathways A, B, and C have been located on the PESs for the reaction of $[Ga_2Mg_2O_5]^{\bullet+}$ with H_2O. All start with the formation of a quite stable encounter complex (**EC**), in which the oxygen atom of water coordinates to one of the Mg atoms of the cluster ion; this step is exothermic by -146 kJ mol^{-1}. Subsequently, in pathway A in the course of lengthening the bond between magnesium and the bridging oxygen atom, the Mg-bound water ligand forms a H bond to the oxygen atom ($O_b{}^-$) that originally bridged the two magnesium atoms ($R_{O_b\text{-}H} = 1.45$ Å) thus generating intermediate **1** (-113 kJ mol^{-1}) via transition state **TS1** (-99 kJ mol^{-1}). Next, cleavage of the O_w–H bond takes place via transition state **TS2** (-89 kJ mol^{-1}) to give rise to intermediate **2** (-97 kJ mol^{-1}) which has two structurally equivalent OH groups. The ejection of either of the OH groups constitutes the rate-limiting step and results in the formation of product **P**, $[Ga_2Mg_2O_5H]^+$, which is -44 kJ mol^{-1} lower in energy than the isolated reactants. Clearly, the overall process is accessible at thermal conditions, in agreement with the experiments, in particular with the labeling experiments with $H_2{}^{18}O$, Figure 1d. Pathway A is by far the most-favored energetically compared to the two alternative routes B and C. For these two processes, high barriers, that is, **TS3** and **TS4**, have to be surmounted; as they are 14 kJ mol^{-1} and 65 kJ mol^{-1} higher in energy than the separated reactants, respectively, they are not accessible under thermal conditions.

As shown in Table 1, **TS2** corresponds to a late transition structure: the HO–H bond ($R_{O_w\text{-}H}$) is elongated by 0.53 Å (from 1.05 Å in **1** to 1.58 Å in **TS2**), and the length of the newly formed O_b–H bond ($R_{O_b\text{-}H}$) is only 1.00 Å in **TS2** (compared to 1.45 Å in **1** and to 0.96 Å in **2**). These bond breaking and bond making processes result in an overall barrier of 24 kJ mol^{-1} relative to **1**. Regarding the structures of the alternative hydrogen-atom abstraction via **TS3** and **TS4**, both transition structures share similar structural properties (see Table 1), yet **TS3** is 51 kJ mol^{-1} lower in energy than **TS4**.

A frontier molecular orbital (FMO) analysis on the electron-density development has been performed to provide further details.[9] Figure 3 shows the detailed

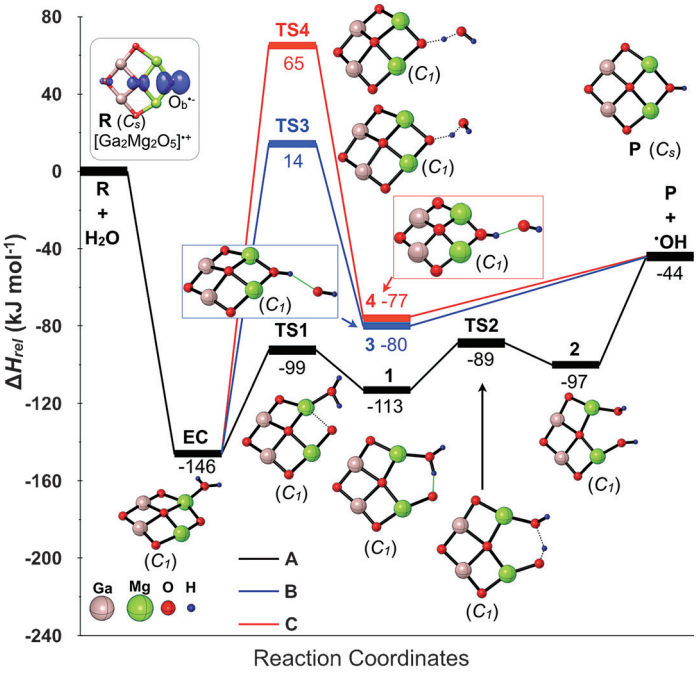

Figure 2. The most favorable potential energy surfaces (kJ mol^{-1}) and key ground-state structures involved in the reaction of $[Ga_2Mg_2O_5]^{\bullet+}$ with H_2O at the G4(MP2)-6X level of theory. Inset: ground-state structure of $[Ga_2Mg_2O_5]^{\bullet+}$. The blue isosurface indicates the AIM-calculated spin-density distribution. For selected geometrical parameters, see Table 1.

Table 1: Geometric parameters of the stationary points involved in the reaction of $[Ga_2Mg_2O_5]^{\bullet+}$ with H_2O as calculated at the BMK/6-31+G-(2df,p) level of theory.[a]

	$R_{Mg\text{-}O_b}$	$R_{O_b\text{-}H}$	$R_{O_w\text{-}H}$	$R_{Mg\text{-}O_w}$	$R_{O_w\text{-}O_b}$	$\measuredangle O_w\text{-}H\text{-}O_b$
R + H_2O	1.93	–	0.96	–	–	–
EC	1.92	3.58	0.96	1.98	3.25	62.6
TS1	2.24	1.53	1.01	1.94	2.35	133.9
1	3.41	1.45	1.05	1.91	2.48	163.4
TS2	3.44	1.00	1.58	1.87	2.33	127.2
2	3.26	0.96	2.31	1.90	2.13	67.4
TS3	1.97	1.32	1.07	3.55	2.22	136.0
TS4	1.97	1.29	1.08	3.64	2.36	166.4
3	1.92	0.96	2.04	4.72	2.86	141.6
4	1.93	0.96	2.01	3.88	2.88	148.9
P + OH	1.93	0.96	–	–	–	–

[a] Bond lengths [Å] and bond angles [°]. O_b indicates the bridging oxygen atom of the cluster ion, and O_w refers to the oxygen atom of water.

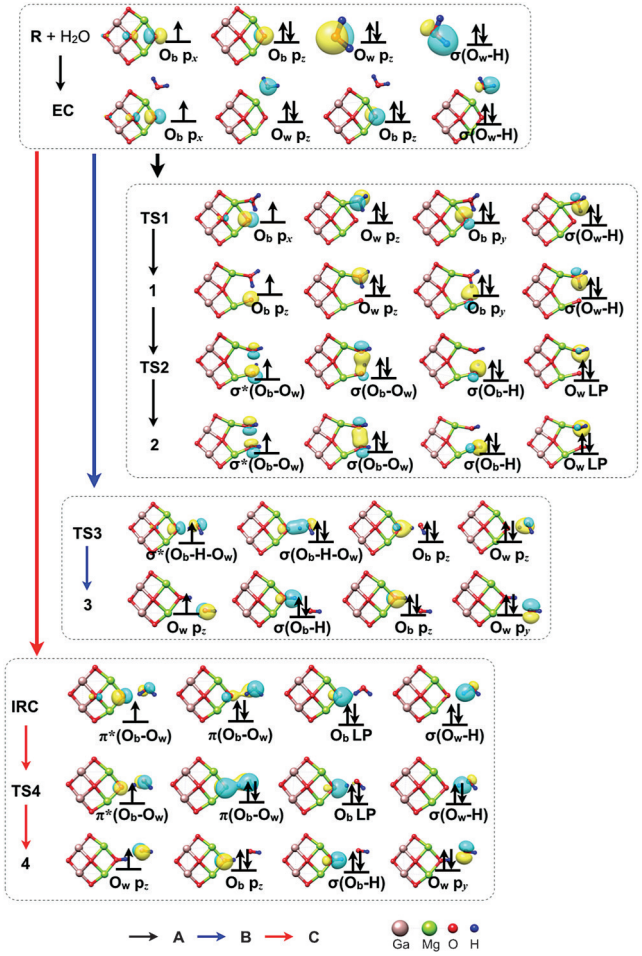

Figure 3. Schematic frontier MO diagrams for the three pathways A, B, and C in the reactions of the $[Ga_2Mg_2O_5]^{\bullet+}/H_2O$ couple. A point from the IRC on the way from **EC** to **TS4** in pathway C is also given to demonstrate the orbital rearrangement, that is, the rotation of the O_b p_x orbital to hybridize with the O_w p_z orbital. See text and Figures S2,S3 for details.

evolution of the electronic structures along the three reaction pathways.

For pathway A, the overall process **1**→**TS2**→**2** can be separated into two events, that is, proton and electron transfers, in which different orbitals are involved. Thus, the electron lone pair (LP) localized at O_b in the p_y orbital in **1** abstracts a proton from the OH group of water and forms a $\sigma(O_b–H)$ bond in **TS2**; accordingly, the electron pair of the former $\sigma(O_w–H)$ bond of the H_2O moiety in **1** is transformed to a lone electron pair on O_w in **TS2**. At the same time, a hybridization of the doubly occupied p_z orbital of O_w, perpendicular to the O-H-O axis, and the singly occupied p_z orbital of O_b is achieved by rotations of the Mg–O_b and Mg–O_w bonds, respectively, giving rise to a doubly occupied $\sigma(O_b–O_w)$ bonding orbital and a singly occupied $\sigma^*(O_b–O_w)$ anti-bonding orbital in **TS2**; thus electron density is transferred to O_b. In going from **TS2** to **2**, the Mg–O_b bond rotates further to achieve a better alignment of the $\sigma^*(O_b–O_w)$ anti-bonding orbital. Apart from that, the electronic structure of **2** is similar to that of **TS2**; this is in line with assigning **TS2** as being a late transition structure as mentioned above. In total, this reaction pathway can be characterized as a proton-coupled electron transfer (PCET).[10]

In contrast, pathway B can be described in terms of a standard hydrogen-atom transfer (HAT) mechanism. As shown in Figure 3, three electrons are delocalized over the O-H-O moiety in transition state **TS3**; one of them originates from the p_x orbital of O_b in **R** and two from the $\sigma(O_w–H)$ bond in H_2O, thus resulting in a 3-electron/3-center transition state characterized by a doubly occupied bonding orbital along the O-H-O axis, $\sigma(O_b\text{-}H\text{-}O_w)$, and a singly occupied anti-bonding orbital, $\sigma^*(O_b\text{-}H\text{-}O_w)$. The electron pair in the p_z orbital of O_b is perpendicular to the O-H-O axis and thus acts as a spectator. These features are consistent with classical HAT mechanism.[10,11]

As mentioned above, pathways B and C have similar features regarding the structural properties. However, a more detailed analysis reveals that pathway C actually corresponds to a PCET rather than a conventional HAT process as identified for pathway B. As shown in Figure 3, in pathway C as the incoming water ligand approaches O_b of the cluster, the singly occupied O_b p_x orbital in **EC** rotates for a better overlap with the doubly occupied O_w p_z to form two orbitals, that is, a doubly occupied $\pi(O_b–O_w)$ orbital and a singly occupied anti-bonding $\pi^*(O_b–O_w)$ orbital in **TS4**. From these two orbitals, the singly occupied O_w p_z orbital and the doubly occupied O_b p_z are generated in intermediate **4**; as a result, an electron has been transferred from the O_w p_z orbital to the O_b p_z orbital. The proton transfer takes place in going from **TS4** to intermediate **4** involving different orbitals: the lone pair at O_b in **TS4** is transformed to the $\sigma(O_b–H)$ bond in **4** while the $\sigma(O_w–H)$ bond in **TS4** is converted into a lone pair at O_w in **4**.[10,12]

As stated earlier, the energetics of the electron donator and electron acceptor orbitals are crucial for the reactivity of metal oxide clusters towards R–H bonds.[9a,e,13] The fundamental difference between pathways B and C can be traced back to different electron-donator orbitals (EDO). The p_x orbital of O_b corresponds to the electron-accepting orbital (EAO) in both pathways; however, the EDO corresponds to the $\sigma(O_w–H)$ orbital in pathway B and to the p_z orbital of O_w in pathway C. This gives rise to a 3-electron/3-center $\sigma(O_b\text{-}H\text{-}O_w)$ and $\sigma^*(O_b\text{-}H\text{-}O_w)$ bond in pathway B while an energetically rather unfavorable 3-electron/3-center with π character, that is, $\pi(O_b–O_w)$ and $\pi^*(O_b–O_w)$, is involved in pathway C. The different O···O interaction is also reflected in a shorter $R_{O\text{-}O}$ distance of 2.22 Å in **TS3** (pathway B) and a longer $R_{O\text{-}O}$ of 2.36 Å in **TS4** (pathway C).

In summary, herein we provide novel mechanistic insight into various reaction pathways of hydrogen-atom transfer from water to the heteronuclear oxide cluster $[Ga_2Mg_2O_5]^{\bullet+}$. The by far most favorable pathway corresponds to a proton-coupled electron transfer (PCET) mechanism, in the course of which two structurally equivalent Mg-(OH) units are formed. A conventional hydrogen-atom transfer (HAT) mechanism, which characterizes the $[Ga_2Mg_2O_5]^{\bullet+}/CH_4/C_2H_6$ couples,[7a] is much more demanding energetically. A second PCET pathway also exits for the $[Ga_2Mg_2O_5]^{\bullet+}/H_2O$ system. Although the transition state of this alternative mechanism

has a structure similar to that of the HAT pathway, the electronic structures are quite different.

Acknowledgements

This research was sponsored by the Deutsche Forschungsgemeinschaft (DFG), in particular the Cluster of Excellence "Unifying Concepts in Catalysis" (coordinated by the Technische Universität Berlin and funded by the DFG), and the Fonds der Chemischen Industrie. J.L. is grateful to "Unicat" for a postdoctoral fellowship. X.-N.W. appreciates support from the Alexander von Humboldt Foundation in the form of a postdoctoral research fellowship. We thank Dr. C. Geng and Dr. T. Weiske for helpful comments.

Keywords: computational chemistry · gas-phase reactions · mass spectrometry · O—H bond cleavage · radicals

How to cite: *Angew. Chem. Int. Ed.* **2015**, *54*, 11861–11864
Angew. Chem. **2015**, *127*, 12028–12032

[1] a) J. Liu, Y. Liu, N. Liu, Y. Han, X. Zhang, H. Huang, Y. Lifshitz, S.-T. Lee, J. Zhong, Z. Kang, *Science* **2015**, *347*, 970–974; b) M. D. Kärkäs, O. Verho, E. V. Johnston, B. Åkermark, *Chem. Rev.* **2014**, *114*, 11863–12001; c) N. Cox, D. A. Pantazis, F. Neese, W. Lubitz, *Acc. Chem. Res.* **2013**, *46*, 1588–1596; d) D. Cappelletti, E. Ronca, L. Belpassi, F. Tarantelli, F. Pirani, *Acc. Chem. Res.* **2012**, *45*, 1571–1580; e) H. Dau, C. Limberg, T. Reier, M. Risch, S. Roggan, P. Strasser, *ChemCatChem* **2010**, *2*, 724–761; f) P. J. Roach, W. H. Woodward, A. W. Castleman, A. C. Reber, S. N. Khanna, *Science* **2009**, *323*, 492–495; g) M. Yagi, M. Kaneko, *Chem. Rev.* **2000**, *100*, 21–36; h) O. Blum, D. Stöckigt, D. Schröder, H. Schwarz, *Angew. Chem. Int. Ed. Engl.* **1992**, *31*, 603–604; *Angew. Chem.* **1992**, *104*, 637–639.

[2] M. G. Walter, E. L. Warren, J. R. McKone, S. W. Boettcher, Q. Mi, E. A. Santori, N. S. Lewis, *Chem. Rev.* **2010**, *110*, 6446–6473.

[3] a) J.-B. Ma, Y.-X. Zhao, S.-G. He, X.-L. Ding, *J. Phys. Chem. A* **2012**, *116*, 2049–2054; b) S. Feyel, D. Schröder, H. Schwarz, *Eur. J. Inorg. Chem.* **2008**, 4961–4967; c) G. K. Koyanagi, D. K. Bohme, I. Kretzschmar, D. Schröder, H. Schwarz, *J. Phys. Chem. A* **2001**, *105*, 4259–4271; d) S. Bärsch, D. Schröder, H. Schwarz, *Chem. Eur. J.* **2000**, *6*, 1789–1796; e) M. Brönstrup, D. Schröder, H. Schwarz, *Chem. Eur. J.* **1999**, *5*, 1176–1185.

[4] X.-F. Yang, A. Wang, B. Qiao, J. Li, J. Liu, T. Zhang, *Acc. Chem. Res.* **2013**, *46*, 1740–1748.

[5] a) R. Horn, R. Schlögl, *Catal. Lett.* **2015**, *145*, 23–39; b) J. Li, P. González-Navarrete, M. Schlangen, H. Schwarz, *Chem. Eur. J.* **2015**, *21*, 7780–7789; c) R. A. J. O'Hair, N. J. Rijs, *Acc. Chem. Res.* **2015**, *48*, 329–340; d) H. Schwarz, *Isr. J. Chem.* **2014**, *54*, 1413–1431; e) Z. Luo, A. W. Castleman, *Acc. Chem. Res.* **2014**, *47*, 2931–2940; f) S. M. Lang, T. M. Bernhardt, *Phys. Chem. Chem. Phys.* **2012**, *14*, 9255–9269; g) S. Yin, E. R. Bernstein, *Int. J. Mass Spectrom.* **2012**, *321–322*, 49–65; h) D. K. Böhme, H. Schwarz, *Angew. Chem. Int. Ed.* **2005**, *44*, 2336–2354; *Angew. Chem.* **2005**, *117*, 2388–2406; i) A. T. Bell, *Science* **2003**, *299*, 1688–1691.

[6] a) J. L. Li, R. A. Mata, U. Ryde, *J. Chem. Theory Comput.* **2013**, *9*, 1799–1807; b) X. Zhang, H. Schwarz, *Theor. Chem. Acc.* **2011**, *129*, 389–399; c) B. Chan, J. Deng, L. Radom, *J. Chem. Theory Comput.* **2010**, *7*, 112–120; d) J. Li, C. Geng, X. Huang, C. Sun, *J. Chem. Theory Comput.* **2006**, *2*, 1551–1564.

[7] a) J. Li, X.-N. Wu, M. Schlangen, S. Zhou, P. González-Navarrete, S. Tang, H. Schwarz, *Angew. Chem. Int. Ed.* **2015**, *54*, 5074–5078; *Angew. Chem.* **2015**, *127*, 5163–5167; b) H. Schwarz, *Angew. Chem. Int. Ed.* **2015**, DOI: 10.1002/anie.201500649; *Angew. Chem.* **2015**, DOI: 10.1002/anie.201500649; c) J. Sauer, H.-J. Freund, *Catal. Lett.* **2015**, *145*, 109–125.

[8] a) G. Kummerlöwe, M. K. Beyer, *Int. J. Mass Spectrom.* **2005**, *244*, 84–90; b) T. Su, M. T. Bowers, *J. Chem. Phys.* **1973**, *58*, 3027–3037; c) M. T. Bowers, J. B. Laudenslager, *J. Chem. Phys.* **1972**, *56*, 4711–4712.

[9] a) X. Sun, C. Geng, R. Huo, U. Ryde, Y. Bu, J. Li, *J. Phys. Chem. B* **2014**, *118*, 1493–1500; b) X. Sun, X. Sun, C. Geng, H. Zhao, J. Li, *J. Phys. Chem. A* **2014**, *118*, 7146–7158; c) J. L. Li, X. Zhang, X. R. Huang, *Phys. Chem. Chem. Phys.* **2012**, *14*, 246–256; d) X. L. Sun, X. R. Huang, J. L. Li, R. P. Huo, C. C. Sun, *J. Phys. Chem. A* **2012**, *116*, 1475–1485; e) C. Y. Geng, S. Ye, F. Neese, *Angew. Chem. Int. Ed.* **2010**, *49*, 5717–5720; *Angew. Chem.* **2010**, *122*, 5853–5856; f) K. Fukui, *Science* **1982**, *218*, 747–754.

[10] W. Lai, C. Li, H. Chen, S. Shaik, *Angew. Chem. Int. Ed.* **2012**, *51*, 5556–5578; *Angew. Chem.* **2012**, *124*, 5652–5676.

[11] a) H. Schwarz, *Chem. Phys. Lett.* **2015**, *629*, 91–101; b) N. Dietl, M. Schlangen, H. Schwarz, *Angew. Chem. Int. Ed.* **2012**, *51*, 5544–5555; *Angew. Chem.* **2012**, *124*, 5638–5650.

[12] a) C. T. Saouma, J. M. Mayer, *Chem. Sci.* **2014**, *5*, 21–31; b) J. M. Mayer, *Acc. Chem. Res.* **2011**, *44*, 36–46.

[13] a) J. Li, X.-N. Wu, S. Zhou, S. Tang, M. Schlangen, H. Schwarz, *Angew. Chem. Int. Ed.* **2015**, *54*, DOI: 10.1002/anie.201503763; *Angew. Chem.* **2015**, *127*, DOI: 10.1002/ange.201503763; b) P. Verma, K. D. Vogiatzis, N. Planas, J. Borycz, D. J. Xiao, J. R. Long, L. Gagliardi, D. G. Truhlar, *J. Am. Chem. Soc.* **2015**, *137*, 5770–5781; c) C. Geng, S. Ye, F. Neese, *Dalton Trans.* **2014**, *43*, 6079–6086; d) S. Ye, F. Neese, *Proc. Natl. Acad. Sci. USA* **2011**, *108*, 1228–1233; e) M. L. Neidig, A. Decker, O. W. Choroba, F. Huang, M. Kavana, G. R. Moran, J. B. Spencer, E. I. Solomon, *Proc. Natl. Acad. Sci. USA* **2006**, *103*, 12966–12973.

Received: June 11, 2015
Published online: August 14, 2015

